

## Manufacturing, high heat flux testing and post mortem analyses of a W-PIM mock-up

Steffen Antusch<sup>a,\*</sup>, Eliseo Visca<sup>b</sup>, Alexander Klein<sup>a</sup>, Heinz Walter<sup>a</sup>, Kilian Pursche<sup>a</sup>, Marius Wirtz<sup>d</sup>, Thorsten Loewenhoff<sup>d</sup>, Henri Greuner<sup>c</sup>, Bernd Böswirth<sup>c</sup>, Jan Hoffmann<sup>a</sup>, Daniel Bolich<sup>a</sup>, Gerald Pintsuk<sup>d</sup>, Michael Rieth<sup>a</sup>

<sup>a</sup> Karlsruhe Institute of Technology, Institute for Applied Materials, Karlsruhe, Germany

<sup>b</sup> Associazione EURATOM-ENEA sulla Fusione, C.R.Frascati, Frascati, Italy

<sup>c</sup> Max-Planck-Institut für Plasmaphysik, Garching, Germany

<sup>d</sup> Forschungszentrum Jülich GmbH, Institute of Energy and Climate Research, Partner of the Trilateral Euregio Cluster (TEC), Jülich, Germany

### ARTICLE INFO

#### Keywords:

Powder Injection Molding (PIM)  
Hot Radial Pressing (HRP)  
Tungsten  
Monoblock  
Mock-up  
HHF testing

### ABSTRACT

In the framework of the European material development programme for fusion power plants beyond the international thermonuclear experimental reactor (ITER), tungsten (W) is an attractive candidate as plasma facing material for future fusion reactors. The selection of tungsten is owing to its physical properties such as the high melting point of 3420 °C, the high strength and thermal conductivity, the low thermal expansion and low erosion rate. Disadvantages are the low ductility and fracture toughness at room temperature, low oxidation resistance, and the manufacturing by mechanical machining such as milling and turning, because it is extremely cost and time intensive.

Powder Injection Molding (PIM) as near-net-shape technology allows the mass production of complex parts, the direct joining of different materials and the development and manufacturing of composite and prototype materials presenting an interesting alternative process route to conventional manufacturing technologies. With its high precision, the PIM process offers the advantage of reduced costs compared to conventional machining. Isotropic materials, good thermal shock resistance, and high shape complexity are typical properties of PIM tungsten.

This contribution describes the fabrication of tungsten monoblocks, in particular for applications in divertor components, via PIM. The assembly to a component (mock-up) was done by Hot Radial Pressing (HRP). Furthermore, this component was characterized by High Heat Flux (HHF) tests at GLADIS and at JUDITH 2, and achieved 1300 cycles @ 20 MW/m<sup>2</sup>.

Post mortem analyses were performed quantifying and qualifying the occurring damage by metallographic and microscopical means. The crystallographic texture was analysed by EBSD measurements. No change in microstructure during testing was observed.

### 1. Introduction

Industrially produced tungsten (W) grades are available in different types of semi-finished products (rods, plates, and sheets). Conditioned by the fabrication route via powder metallurgy (powder compaction, sintering, rolling or forging) the products are characterized by high density and large quantity. But the subsequent mechanical machining is very time and cost intensive. An alternative mass fabrication method is Powder Injection Molding (PIM). This is a time and cost effective near-net-shape forming process that allows complex shapes and a relatively

high final density [1,2].

The divertor concept of the world largest fusion experiment presently under construction, the International Thermonuclear Experimental Reactor (ITER), is based on tungsten monoblocks as plasma facing material which are connected to CuCrZr-pipes by using different manufacturing technologies (brazing, Hot Isostatic Pressing (HIP), or Hot Radial Pressing (HRP)) [3]. An additional requirement (to keep the components performance as high as possible) is to perform the joining process in such a way that the material properties are not altered. To qualify the involved processes and materials, small units of

\* Corresponding author.

E-mail address: [steffen.antusch@kit.edu](mailto:steffen.antusch@kit.edu) (S. Antusch).

<https://doi.org/10.1016/j.nme.2019.100688>

Received 18 April 2019; Received in revised form 15 May 2019; Accepted 15 May 2019

Available online 24 May 2019

2352-1791/© 2019 The Authors. Published by Elsevier Ltd. This is an open access article under the CC BY license (<http://creativecommons.org/licenses/by/4.0/>).

the real component are fabricated (so-called mock-ups). Then the performance of these mock-ups is determined by high heat flux (HHF) tests [4].

This contribution presents investigations on pure tungsten materials. First, the manufacturing process of the monoblocks by W-PIM and the fabrication to a mock-up by HRP are reported. The high heat flux testing section describes the testing of this mock-up: first in the neutral beam facility GLADIS followed by a second test with the electron beam facility JUDITH 2. The results of the post mortem analysis are briefly discussed and suggestions for further investigations are highlighted.

## 2. Manufacturing

### 2.1. Powder Injection Molding of tungsten monoblocks

The used tungsten powder (> 99.97 wt% W) was mixed with a small quantity of a polymer (binder). The finished granulated so-called feedstock was used for injection molding of green parts. After shaping the green parts, the binder was extracted. The final sintering at temperatures above > 2000 °C leads to a density higher than 98%. This process is very time and cost effective. Isotropic materials, equiaxed grain orientation, good thermal shock resistance, and a high possible shape complexity are typical properties of powder injection molded tungsten [5,6]. Monoblock surface shaping is a key question in the design of plasma facing units [7]. Fig. 1 shows W-PIM monoblocks with various sizes and shapes.

The external dimensions of the produced and used monoblocks were 26 mm x 26 mm x 12 mm. The diameter of the bore in the center was 17 mm.

### 2.2. Fabrication of a W-PIM mock-up via HRP

At first, the W-PIM monoblocks had to be equipped with a copper cast interlayer. The thickness of this interlayer was 1 mm. CuCrZr was used as cooling tube material. The tube inner diameter was 12 mm and the wall thickness 1.5 mm. The mock-up consisted of 4 W-PIM monoblocks, with 0.4 mm gaps in between. Fig. 2 schematically shows all dimensions of the mock-up. The manufacturing of the mock-ups was done by Hot Radial Pressing (HRP) under the following conditions [8,9]:

- Vacuum environment with pressure lower than  $10^{-5}$  mbar.
- Bonding internal tube pressure of 60 MPa.
- Bonding temperature of 580 °C.

- Pressure holding time of 120 min

The W-PIM mock-up was controlled by ultrasonic testing after the HRP manufacturing (see Fig. 3). The figure shows the ultrasonic C-scan image of the mock-up illustrating that it presents a perfect joining quality (blue zones). Ultrasonic C-scan is the representation of the signal amplitude where blue color represents a sound transmission corresponding to a good joining between pipe and monoblock copper interlayer. Only a small circular detached zone (yellow) with a diameter size less of 2 mm is detected. For the enhancement of the water-cooling heat transfer capability a twisted tape (swirl) was installed to promote turbulence. High heat flux testing was done consecutively in two different facilities and on two different, but due to the geometric symmetry of the component equivalent, surfaces of the mock-up: first area (1) exposed in the facility GLADIS, second area (2) tested in JUDITH 2 (see Fig. 4).

## 3. High heat flux testing

### 3.1. HHF testing at GLADIS

The first high heat flux testing was conducted using the neutral beam facility at IPP Garching, which is called Garching LArge Divertor Sample test facility (GLADIS). This facility serves for investigating the thermo-mechanical behavior of components subjected to extreme thermal loading, and is equipped with two 1 MW neutral beam sources for homogeneous heating of plasma facing components at heat fluxes up to 45 MW/m<sup>2</sup> per source and 45 s pulse length [10]. The aim of the HHF tests of the pure W-PIM mock-up was to determine the thermo-mechanical behavior (including the temporally-resolved surface temperature evolution during screening and cycling). Some pre-tests on the PIM material showed already promising results [2,11]. The initial test was done using room temperature water-cooling conditions ( $T_{in} = 20$  °C, 12 m/s axial velocity) and started with a screening from 6 to 25 MW/m<sup>2</sup>, each pulse 10 s loading, followed by 200 cycles at 20 MW/m<sup>2</sup>, 10 s. Fig. 5 shows the infrared images of the mock-up during the screening at 25 MW/m<sup>2</sup>. The screening and cycling at room temperature cooling conditions was performed without any indication of cracks.

The second test campaign was performed similar to DEMO hot water-cooling conditions ( $T_{in} = 130$  °C,  $p_{in} = 40$  bar,  $v = 16$  m/s) with a heat flux of 20 MW/m<sup>2</sup> up to 100 cycles for 10 s. The visual inspection showed one thin crack on the outer edge of one monoblock (see Fig. 6). Next, the mock-up was sent to Forschungszentrum Jülich to continue the high heat flux testing.



Fig. 1. Monoblocks in manifold designs produced via W-PIM. Chamfer (with or without), position and size of bore (center or outboard), thickness (thick or thin) – all these parameters may be varied within certain limits by the use of an adaptable PIM tool.

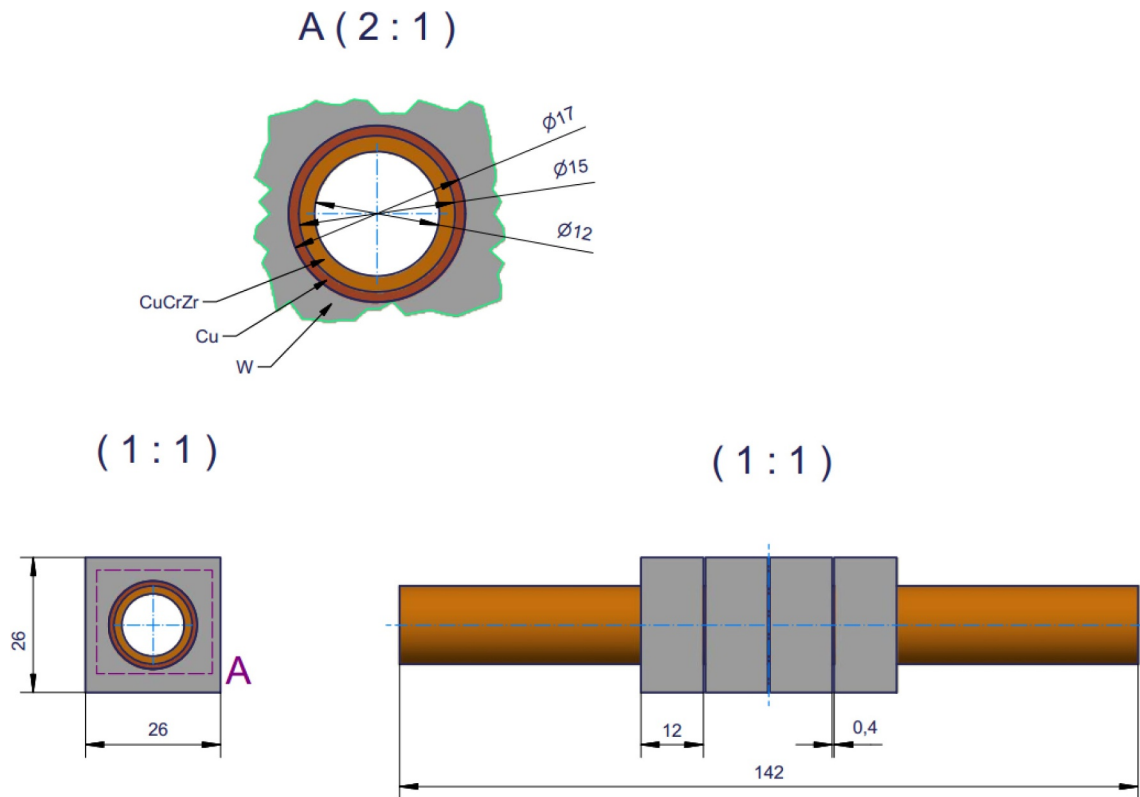


Fig. 2. Dimensions of the W-PIM mock-up (schematically).

### 3.2. Thermal fatigue testing at JUDITH 2

At Forschungszentrum Jülich high heat flux tests with the electron beam facility JUDITH 2 were performed [12]. Pre-tests on pure tungsten materials were very promising [13]. The heat load tests were performed with hot water-cooling similar to ITER conditions ( $T_{in} = 70\text{ }^{\circ}\text{C}$ ,  $p_{in} = 30\text{ bar}$ ,  $v = 11.5\text{ m/s}$ ) applying 100 cycles of  $10\text{ MW/m}^2$  and 1000 cycles of  $20\text{ MW/m}^2$ . Due to inappropriate covering of the surface by the electron beam (i.e., block 4 was only partially loaded), the absorbed power density on blocks 1–3 (measured by water calorimetry) was calculated to about  $\sim 22\text{ MW/m}^2$ . Based on IR-images taken at the end of each loading cycle (assumption emissivity 0.2), at  $10\text{ MW/m}^2$  the temperature of block 2 and 3 is at  $800\text{--}820\text{ }^{\circ}\text{C}$  (at the beginning) and after 100 cycles  $820\text{--}840\text{ }^{\circ}\text{C}$ . At  $20\text{ MW/m}^2$  the measured temperature using the same parameters is between  $2220$  and  $2280\text{ }^{\circ}\text{C}$ . This temperature stays constant till 300 cycles. Between 300 and 1000 cycles the measured temperature using the same parameters continuously increases, while the cooling down performance does not change. Accordingly, this change in measured temperature can be related to an emissivity increase due to the surface roughening by thermal induced damage (i.e. loss of grains).

## 4. Post mortem analyses

### 4.1. Microstructure

Fig. 7 shows the mock-up after high heat flux testing.

Monoblock # 3 showed one crack on the top surface (testing area) with a depth of  $3.4\text{ mm}$ . The cross section in Fig. 7 showed that it is still  $> 1\text{ mm}$  away from the cooling tube. Between block 1 and 2 flaws in the Cu-interlayer were found which might be a result of the high heat flux tests but could also be a pre-existing defect considering the location and the difficulty of detection of such imperfections via non-destructive means prior to testing. However, the CuCrZr tube showed no damage of

any kind (Fig. 8).

### 4.2. Crystallographic texture (EBSD)

Electron backscatter diffraction (EBSD) is a powerful microstructural characterization tool in combination with SEM and allows descriptive analyses of the grain size, orientation, distribution, and form. Fig. 9 shows the initial state and Fig. 10 the microstructure after HHF testing. Both tested surfaces (GLADIS and JUDITH 2 tests) are visible in the EBSD map in Fig. 10. While we see a change in the surface morphology after testing in JUDITH 2, no damage is visible after the tests in GLADIS. This becomes especially apparent when comparing to Fig. 9 where the initial state shows the same microstructural properties. The grain size and state of the microstructure (here: recrystallized state) does not change after both HHF tests. A fine-grained layer on the outer surface which is followed by columnar grains towards the inner material is visible in all states. The gradients visible inside the columnar grains in Fig. 9 result from polishing and not from deformation due to the manufacturing process.

A change of the microstructure in the state before and after HHF testing could not be detected on the whole loaded surface. The clearly visible seam near the surface consists of a  $500\text{ }\mu\text{m}$  thick columnar grain structure. The seam with large columnar grains have a width of approximately  $350\text{--}400\text{ }\mu\text{m}$ , with an average grain size of the elongated grains of about  $160 \times 350\text{--}400\text{ }\mu\text{m}$ . Directly visible on the surface is a thin layer (1–5 grains) with isotropic grain size ( $50\text{--}80\text{ }\mu\text{m}$ ). This microstructure is identical for the whole monoblock, i.e. central areas (see Fig. 7), edges (see also Figs. 7 and 10) and also the unloaded surfaces (see Fig. 9). The authors conclude that the columnar structure is an artefact of the sintering process. In any case, a change in the grain size and structure is not visible. The microstructure of the center is visible in Fig. 7. It's no change in grain structure after GLADIS and JUDITH 2 tests visible. But clearly seen in Fig. 10: No change on the surface morphology after HHF testing in GLADIS - but changing in surface

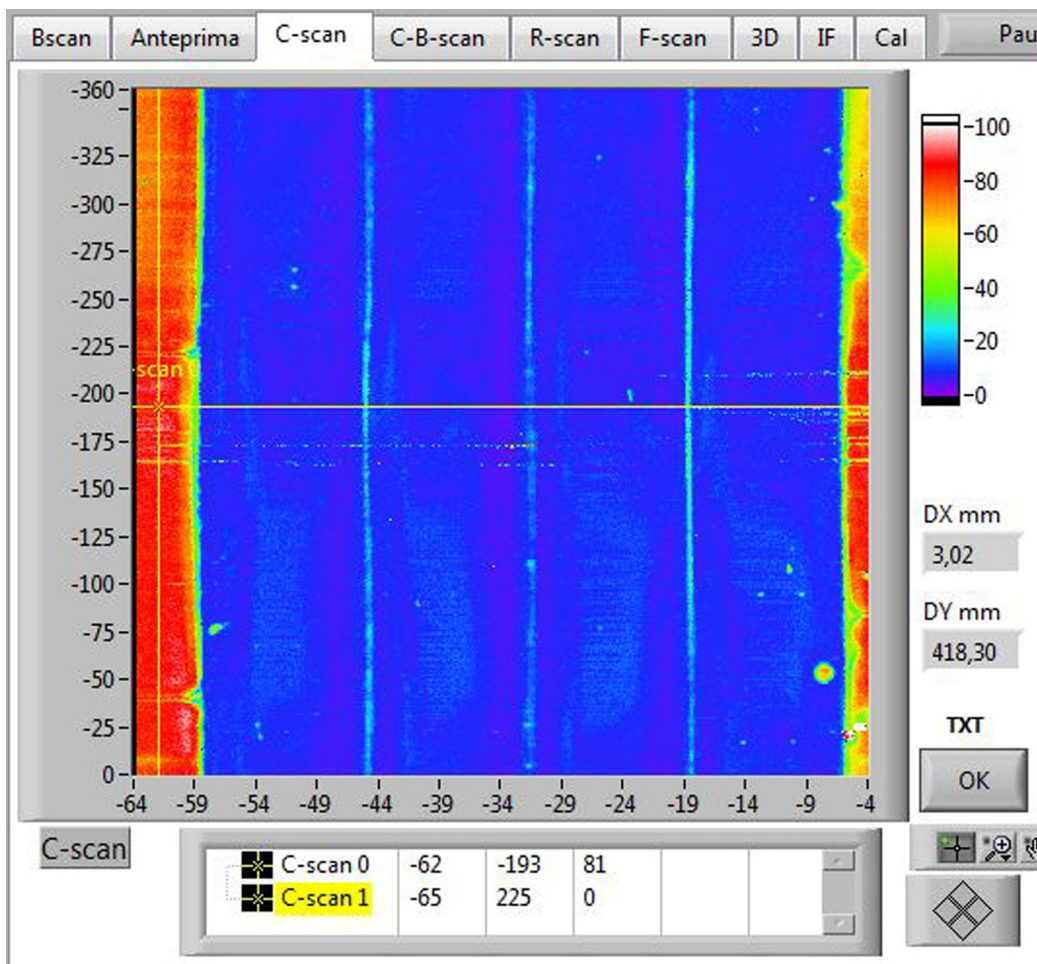
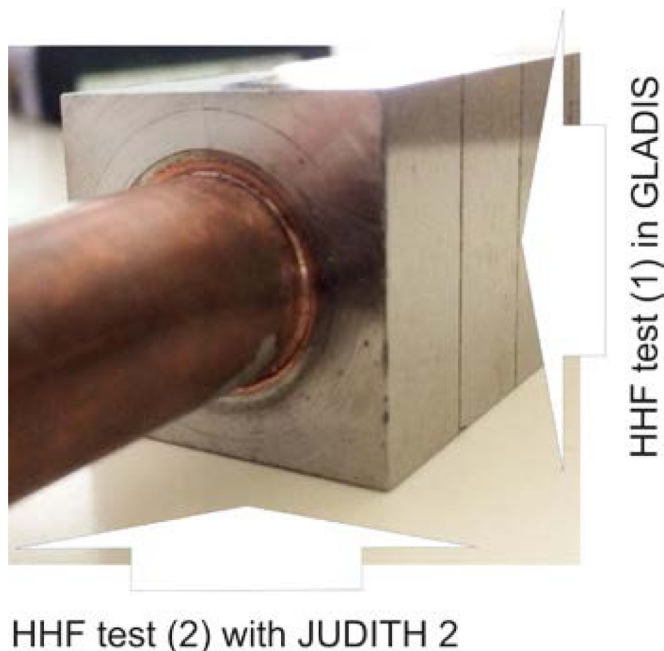


Fig. 3. C-scan of the W-PIM mock-up.



HHF test (2) with JUDITH 2

Fig. 4. Order and area of HHF testing.

morphology (increased surface roughening due to the loss of some grains) after HHF testing with JUDITH 2.

For armor cracking the plastic deformation produced on the loading surface plays a main role. During HHF loading the surface region is stressed under compression by thermal expansion due an extreme temperature gradient. The mechanism of deep and surface cracking by a heat flux load of 20 MW/m<sup>2</sup> is reported in [14].

### 5. Conclusions and outlook

This experimental study demonstrates that the manufacturing techniques PIM and HRP can be successfully applied to divertor component fabrication:

- Monoblocks (26 × 26 × 12 mm) produced via PIM
- Assembly to a mock-up by HRP
- HHF testing at GLADIS: Screening up to 25 MW/m<sup>2</sup>
- HHF testing at GLADIS: 300 cycles @ 20 MW/m<sup>2</sup>
- HHF testing at JUDITH 2: 100 cycles @ 10 MW/m<sup>2</sup>
- HHF testing at JUDITH 2: 1000 cycles @ 20 MW/m<sup>2</sup>
- No change in microstructure during testing
- No recrystallization
- One surface crack

The presence of melting zones between the tungsten blocks and the copper interlayer zone and the formation of surface cracks need to be investigated in more detail in future test series. Particle formation can be easily implemented in the PIM process, which has an enormous



Fig. 5. Infrared (IR) image of the mock-up during the screening.

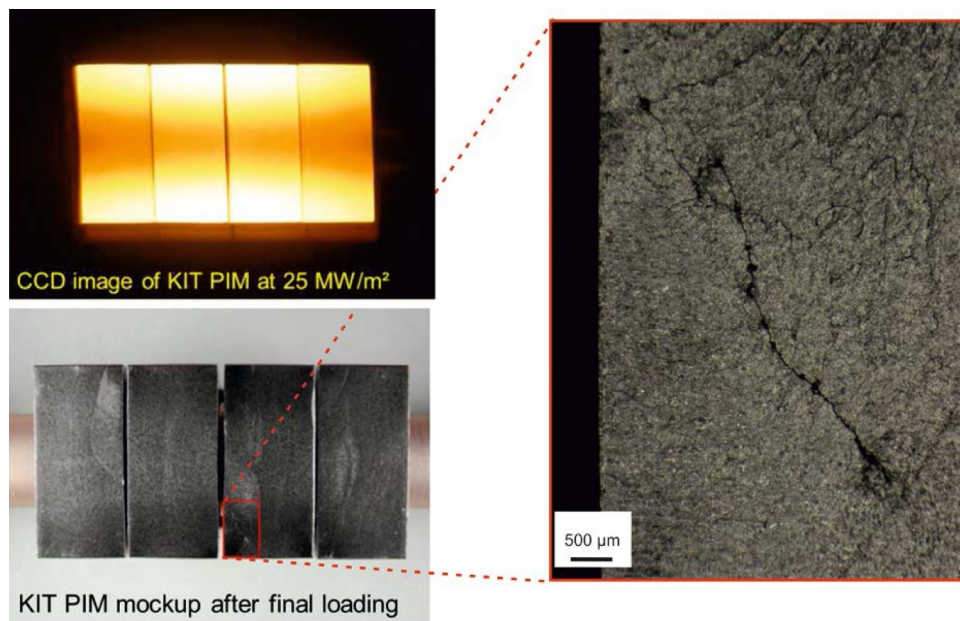


Fig. 6. W-PIM mock-up after final loading at GLADIS, small surface crack on one monoblock.

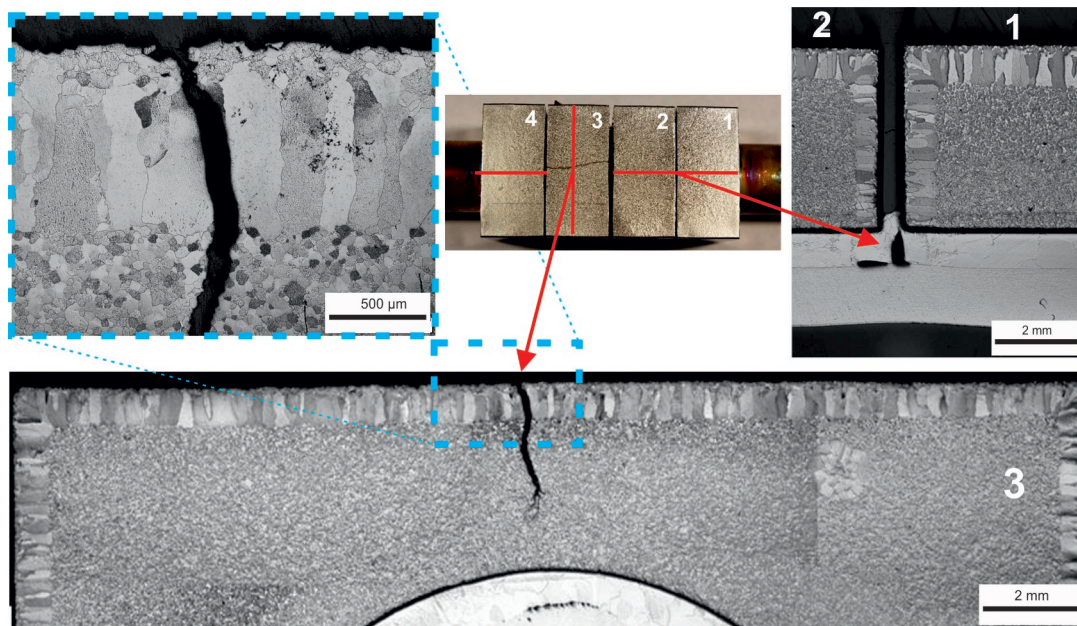


Fig. 7. W-PIM mock-up after final loading at JUDITH 2, one crack on monoblock #3.

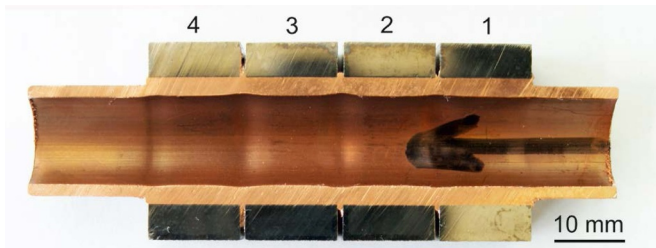


Fig. 8. Cross-section of the W-PIM mock-up after HHF testing. The arrow (right) marked the flow direction of the cooling water.

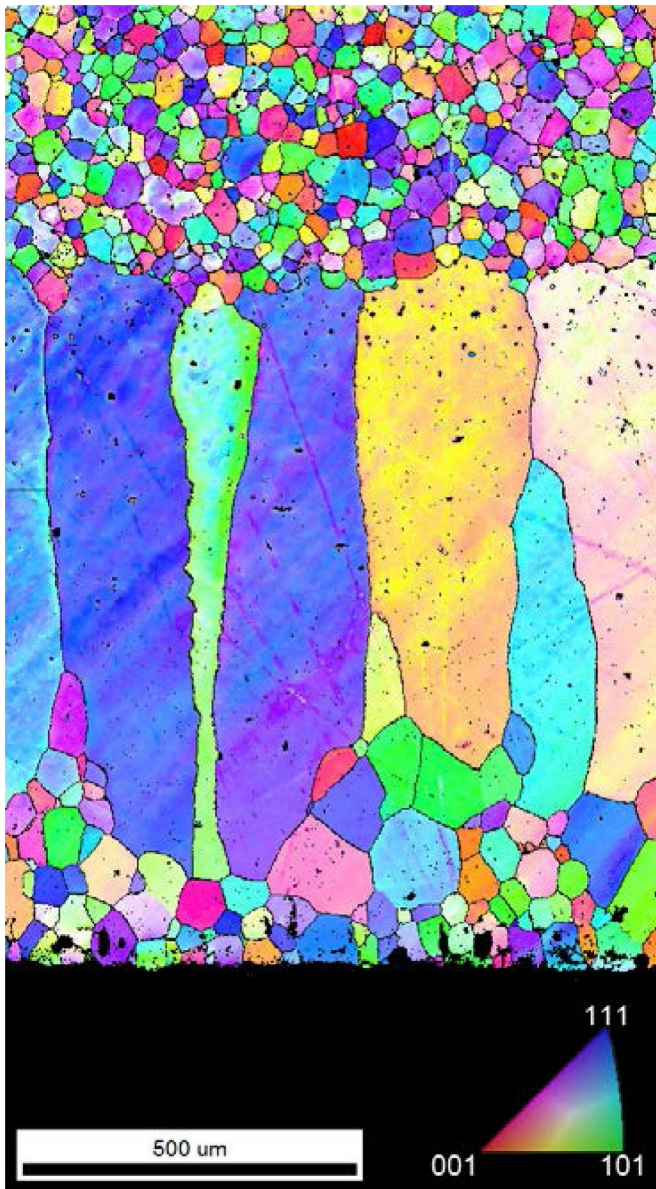


Fig. 9. Initial state (IPF grains).

effect on the material properties [15,16]. A side effect of particle introduction is the suppression of the columnar grain structure (seam). Therefore, the performance of particle reinforced tungsten composites, like for example W-TiC will be investigated in similar mock-ups in the near future.

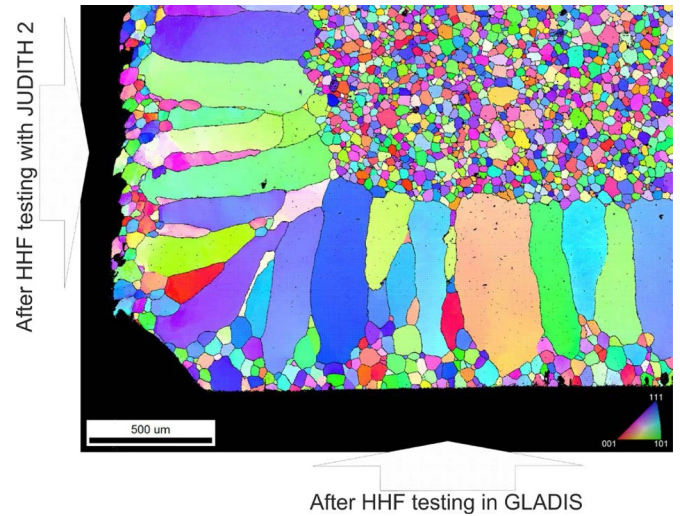


Fig. 10. Left: after testing with JUDITH 2, bottom: after testing in GLADIS (IPF grains).

#### Declaration of Competing Interest

None.

#### Acknowledgments

This work has been carried out within the framework of the EUROfusion Consortium and has received funding from the Euratom research and training programme 2014–2018 and 2019–2020 under grant agreement no 633053. The views and opinions expressed herein do not necessarily reflect those of the European Commission. The authors are grateful to all their colleagues at the Karlsruhe Institute of Technology, Forschungszentrum Jülich, ENEA and Mrs. Gabriele Matern and Dr. Hans Maier at IPP Garching for the support and fruitful discussions. Dr. Wolfram Knabl from PLANSEE SE and Mrs. Mirjam Hoffmann from KIT are especially acknowledged for their contributions.

#### References

- [1] S. Antusch, L. Commin, M. Müller, V. Plotter, T. Weingaertner, Two component tungsten Powder Injection Molding – an effective mass production process, *J. Nucl. Mater.* 447 (2014) 314–317.
- [2] S. Antusch, D.E.J. Armstrong, T.B. Britton, L. Commin, J.S.K.-L. Gibson, H. Greuner, J. Hoffmann, W. Knabl, G. Pintsuk, M. Rieth, S.G. Roberts, T. Weingaertner, Mechanical and microstructural investigations of tungsten and doped tungsten materials produced via Powder Injection Molding, *Nucl. Mater. Energy* 3–4 (2015) 22–31.
- [3] M. Merola, D. Loesser, A. Martin, P. Chappuis, R. Mitteau, V. Komarov, R.A. Pitts, S. Gicquel, V. Barabash, L. Giancarli, J. Palmer, M. Nakahira, A. Loarte, D. Campbell, R. Eaton, A. Kukushkin, M. Sugihara, F. Zhang, C.S. Kim, R. Raffray, L. Ferrand, D. Yao, S. Sadakov, A. Furmanek, V. Rozov, T. Hirai, F. Escourbiac, T. Jokinen, B. Calcagno, S. Mori, ITER plasma-facing components, *Fusion Eng. Des.* 85 (2010) 2312–2322.
- [4] J.H. You, E. Visca, T. Barrett, B. Bösowirh, F. Crescenzi, F. Domptail, M. Fursdon, F. Gallay, B-E. Ghidersa, H. Greuner, M. Li, A.v. Müller, J. Reiser, M. Richou, S. Roccella, Ch. Vorpahl, European divertor target concepts for DEMO: design rationales and high heat flux performance, *Nucl. Mater. Energy* 16 (2018) 1–11.
- [5] G. Pintsuk, M. Rieth, M. Wirtz, Manufacturing and characterization of PIM-W materials as plasma facing materials, *Phys. Scr.* T167 (2016) 014056.
- [6] S. Antusch, J. Reiser, J. Hoffmann, A. Onea, Refractory materials for energy applications, *Energy Technol.* 5 (2017) 1064–1070.
- [7] R.A. Pitts, S. Bardin, B. Bazylev, M.A. van den Berg, P. Bunting, S. Carpentier-Chouchana, J.W. Coenen, Y. Corre, R. Dejarnac, F. Escourbiac, J. Gaspar, J.P. Gunn, T. Hirai, S-H. Hong, J. Horacek, D. Iglesias, M. Komm, K. Krieger, C. Lasnier, G.F. Matthews, T.W. Morgan, S. Panayotis, S. Pestchanyi, A. Podolnik, R.E. Nygren, D.L. Rudakov, G. De Temmerman, P. Vondracek, J.G. Watkins, Physics conclusions in support of ITER W divertor monoblock shaping, *Nucl. Mater. Energy* 12 (2017) 60–74.
- [8] E. Visca, E. Cacciotti, A. Komarov, S. Libera, N. Litunovsky, A. Makhonov, A. Mancini, M. Merola, A. Pizzuto, B. Riccardi, S. Roccella, Manufacturing, testing

- and post-test examination of ITER divertor vertical target W small scale mock-ups, *Fusion Eng. Des.* 86 (2011) 1591–1594.
- [9] E. Visca, S. Libera, A. Mancini, G. Mazzone, A. Pizzuto, C. Testani, Hot Radial Pressing, an alternative technique for the manufacturing of plasma-facing components, *Fusion Eng. Des.* 75–79 (2005) 485–489.
- [10] H. Greuner, B. Boeswirth, J. Boscary, P. McNeely, et al., High heat flux facility GLADIS: operational characteristics and results of W7-X pre-series target tests, *J. Nucl. Mater.* 367–370 (2007) 1444–1448.
- [11] H. Greuner, H. Maier, M. Balden, Ch. Linsmeier, B. Böswirth, S. Lindig, P. Norajitra, S. Antusch, M. Rieth, Investigation of European W materials exposed to high heat flux H/He neutral beams, *J. Nucl. Mater.* 442 (2013) 256–260.
- [12] P. Majerus, R. Duwe, T. Hirai, W. Kühnlein, J. Linke, M. Rödiger, The new electron beam test facility JUDITH II for high heat flux experiments on plasma facing components, *Fusion Eng. Des.* 75–79 (2005) 365–369.
- [13] G. Pintsuk, M. Wirtz, S. Antusch, T. Weingärtner, Recrystallization and composition dependent thermal fatigue response of different tungsten grades, *Int. J. Refract. Met. Hard Mater.* 72 (2018) 97–103.
- [14] M. Li, J.-H. You, Design options to mitigate deep cracking of tungsten armor, *Fusion Eng. Des.* 124 (2017) 468–472.
- [15] S. Antusch, J. Hoffmann, A. Klein, J.P. Gunn, M. Rieth, T. Weingaertner, Processing of complex near-net-shaped tungsten parts by PIM, *Nucl. Mater. Energy* 16 (2018) 71–75.
- [16] C. Yin, D. Terentyev, T. Pardoën, A. Bakaeva, R. Petrov, S. Antusch, M. Rieth, M. Vilémová, J. Matějčíček, T. Zhang, Tensile properties of baseline and advanced tungsten grades for fusion applications, *Int. J. Refract. Met. Hard Mater.* 75 (2018) 153–162.